



HAL
open science

Reclamation of forward osmosis reject water containing hexavalent chromium via coupled electrochemical-physical processes

Milad Mousazadeh, Zohreh Naghdali, Işık Kabdaşlı, Miguel A Sandoval, Fatima Ezzahra Titchou, Farideh Malekdar, Mahmoud Nasr, Carlos A Martínez-Huitle, Eric Lichtfouse, Mohammad Mahdi Emamjomeh

► To cite this version:

Milad Mousazadeh, Zohreh Naghdali, Işık Kabdaşlı, Miguel A Sandoval, Fatima Ezzahra Titchou, et al.. Reclamation of forward osmosis reject water containing hexavalent chromium via coupled electrochemical-physical processes. *Environmental Technology*, 2024, 45, pp.888-901. 10.1080/09593330.2022.2130104 . hal-03816196

HAL Id: hal-03816196

<https://hal.science/hal-03816196>

Submitted on 15 Oct 2022

HAL is a multi-disciplinary open access archive for the deposit and dissemination of scientific research documents, whether they are published or not. The documents may come from teaching and research institutions in France or abroad, or from public or private research centers.

L'archive ouverte pluridisciplinaire **HAL**, est destinée au dépôt et à la diffusion de documents scientifiques de niveau recherche, publiés ou non, émanant des établissements d'enseignement et de recherche français ou étrangers, des laboratoires publics ou privés.

Reclamation of forward osmosis reject water containing hexavalent chromium via coupled electrochemical-physical processes

Milad Mousazadeh ^{1,2,3,*}, Zohreh Naghdali ^{1,2}, Işık Kabdaşlı ^{3,*}, Miguel A. Sandoval ^{4,5,*}, Fatima Ezzahra Titchou ⁶, Farideh Malekdar ⁷, Mahmoud Nasr ^{8,9}, Carlos A. Martínez-Huitle ¹⁰, Eric Lichtfouse ¹¹ and Mohammad Mahdi Emamjomeh ¹²

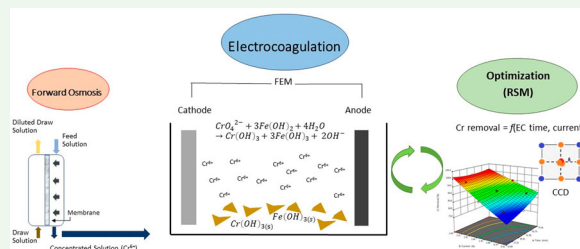
¹Social Determinants of Health Research Center, Research Institute for Prevention of Non-Communicable Diseases, Qazvin University of Medical Sciences, Qazvin, Iran; ²Department of Environmental Health Engineering, School of Health, Qazvin University of Medical Sciences, Qazvin, Iran; ³Civil Engineering Faculty, Environmental Engineering Department, İstanbul Technical University, İstanbul, Republic of Turkey; ⁴Facultad de Química y Biología, Laboratorio de Electroquímica Medio Ambiental, LEQMA, Universidad de Santiago de Chile USACH, Santiago, Chile; ⁵División de Ciencias Naturales y Exactas, Departamento de Ingeniería Química, Universidad de Guanajuato, Guanajuato, Mexico; ⁶Faculty of Sciences, Chemical Department, Ibn Zohr University, Agadir, Morocco; ⁷Department of Chemical and Petroleum Engineering, Sharif University of Technology, Tehran, Iran; ⁸Environmental Engineering Department, Egypt-Japan University of Science and Technology (E-JUST), New Borg El-Arab City, Egypt; ⁹Sanitary Engineering Department, Faculty of Engineering, Alexandria University, Alexandria, Egypt; ¹⁰Institute of Chemistry, Environmental and Applied Electrochemical Laboratory, Federal University of Rio Grande Do Norte, Natal, Brazil; ¹¹CNRS, IRD, INRAE, Coll France, CEREGE, Aix-Marseille Univ, Marseille, France

ABSTRACT

Forward osmosis is a water separation process that uses the natural energy of osmotic pressure to separate water from dissolved solutes through a semipermeable membrane. One of the major challenges using this process is the rejection water which contains high content of pollutants, hindering its practical application. Herein, for the first time, this work introduces a coupled electrochemical-physical process including iron-electrocoagulation/filtration/sedimentation as a cost-effective treatment to the forward osmosis reject water containing hexavalent chromium to be reclaimed. The synergistic treatment was optimized through a central composite design and response surface methodology to enhance hexavalent Cr removal and minimize operating costs, electrical energy consumption, and settled sludge volume. A 90.0% chromium removal was achieved under optimized conditions: electrolysis time of 59.7 min and current of 1.24 A ($J = 6.32 \text{ mA cm}^{-2}$). In addition, operating costs of 0.014 USD m^{-3} , electrical energy consumption of 0.005 kWh m^{-3} , and settled sludge volume of 445 mL L^{-1} were obtained.

KEYWORDS

Hexavalent chromium removal; Electrocoagulation; Forward osmosis concentrate; Response surface methodology; Sustainable treatment



Highlights

- Forward osmosis reject (FOR) wastewater was treated through Fe-EC/filtration/sedimentation processes.
- Chromium (Cr(VI)+Cr(III)) removal was achieved from FOR by Fe-EC/filtration/sedimentation processes.
- Critical parameters namely applied current and electrolysis time were optimized.

- A 90% chromium removal was obtained under the most economical conditions of central composite design optimization.

1. Introduction

Heavy metal pollution has been associated with mining and industrial activities [1–4]. Among these metals,

CONTACT Milad Mousazadeh [✉] m_emamjomeh@yahoo.com [✉] Social Determinants of Health Research Center, Research Institute for Prevention of Non-Communicable Diseases, Qazvin University of Medical Sciences, Qazvin, Iran

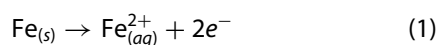
*Co-first author: Milad Mousazadeh, Işık Kabdaşlı, and Miguel A. Sandoval contributed equally to this work.

hexavalent chromium (Cr(VI)) is one of the most concerning pollutants due to its hazardous effects to human beings and environmental health. Cr(VI) can be present in water matrices as monomeric ions H_2CrO_4^0 , HCrO_4^- , and CrO_4^{2-} ; or as the dimeric ion $\text{Cr}_2\text{O}_7^{2-}$ [5]. These oxyanions are the most toxic species of chromium. They have been associated with irreparable harms including mutagenic, teratogenic, carcinogenic, reproductive and birth defects. Moreover, kidney and liver disorders, dermatitis, ulcers and other health effects have been linked to the chronic exposure of wastewater containing high concentrations of Cr(VI). Consequently, the World Health Organization advised a maximum concentration level of 0.05 mg L^{-1} [6, 7]. Wastewaters produced by different industrial processes may contain Cr(VI), therefore, they need to be strictly regulated and treated before discharge to the environment [2, 3]. Some technologies such as membrane-based processes and electrochemical techniques have been developed to meet permissible limit. However, as individual processes, some limitations are worth noting [1,4,8–10].

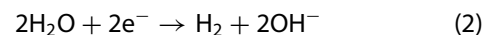
Forward osmosis (FO) is a membrane separation technology with increasing attention for water treatment [11–14]. FO is an osmotically driven membrane process which occurs in a spontaneous manner without requiring hydraulic pressure [15]. The concentration gradient provides a osmotic pressure difference between concentrated draw solution (DS) and diluted feed solution (FS) across a semi-permeable membrane [11,16]. Thus, FO requires lower energy than conventional reverse osmosis and barely experiences fouling issues [15]. However, challenges arise from the reject water handling that contains a high content of pollutants. The removal of pollutants from the FS is an urgent issue to ensure competitive deployment of FO technology. Furthermore, highly concentrated impurities in the forward osmosis reject water (FOR) can cause fouling of the membrane, which requires frequent chemical cleaning. Even though electrocoagulation (EC) can experience challenges to treat diluted chromium effluents [17], it arises as an electrified process that can effectively treat FOR. Electrocoagulation is an electrochemical technology that removes target pollutants from water matrices based on coagulation principles. This technique relies on the use of sacrificial electrodes which provide coagulant species (i.e. Fe^{2+} , Fe^{3+} , Al^{3+}). The coagulant dose is controlled by the applied current. The electrochemical reactions occurring in an EC reactor, with iron material used as sacrificial electrode, are stated as follows [18]:

At the anode:

Fe is oxidized to ferrous iron:

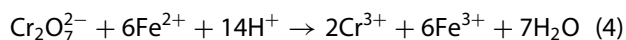
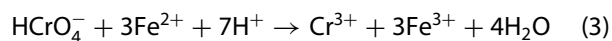


Meanwhile, at the cathode OH^- and H_2 are generated from the water reduction reaction:

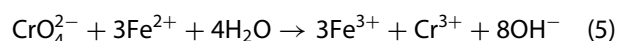


In the reaction solution, hexavalent chromium is reduced to trivalent chromium by dissolved ferrous ions as follows [19,20].

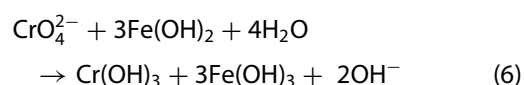
At $\text{pH} < 6.5$:



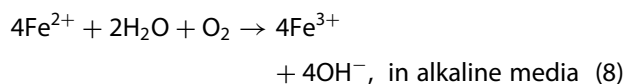
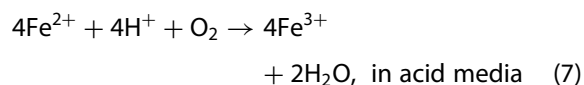
At $6.5 < \text{pH} < 7.5$:



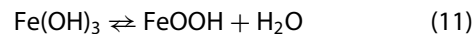
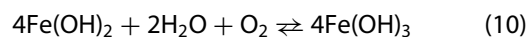
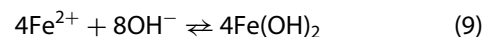
At $\text{pH} > 7.5$:



Additionally, Fe^{3+} may be generated when ferrous ions react with the dissolved oxygen:



In the bulk solution, insoluble iron species $\text{Fe}(\text{OH})_2$, $\text{Fe}(\text{OH})_3$, and/or FeOOH (goethite) are produced according to Equations (9)–(11), respectively.



These dissoluble iron hydroxides favour the formation of flocs. However, ferric oxyhydroxide and goethite are considered the preferent coagulants to remove chromium because these species precipitate in a greater interval of the pH value [19,20].

Trivalent chromium combines with hydroxyl ions to form chromium hydroxide ($\text{Cr}(\text{OH})_3$) which precipitate as amorphous solids. In addition, negative chromium species might adsorb on the positively charged metal hydroxide [21]. Moreover, trivalent chromium removal may occur through other means as well, such as adsorption onto ferric oxyhydroxide and goethite.

Despite the potential benefits of the FO treatment process, this interesting technique suffers from reject water handling that contains a high content of pollutants. According to the literature, it is one of the main challenges that prevents its practical application. Here,

for the first time, this work studies as proof of concept the performance of the iron-electrocoagulation/filtration/sedimentation (Fe-EC/filtration/sedimentation) process to deal with the environmental issue caused by FOR. The Fe-EC module was optimized through experimental design and modelling by the response surface methodology to reclaim FOR with chromium residues. Engineering figures of merit were used to optimize technology competitiveness in terms of key indicators such as chromium removal, electrical energy consumption, operating cost and settled sludge volume.

2. Experimental

2.1. Forward osmosis reject water

FOR was obtained after the forward osmosis process which used a commercial aquaporin-based biomimetic polymeric membrane (Aquaporin Asia Pte. Ltd, Singapore). This process was performed in our previous work to treat a solution containing dichromate potassium [22]. The composition of the obtained feed solution includes CaCl_2 , KCl and MgCl_2 were 0.012, 0.007 and 0.01 mg L^{-1} , respectively. The initial concentration of Cr(VI) in reject water (as feed solution or concentrated solution) was 69 mg L^{-1} . The pH value and the electrical conductivity were 7.1 and 18 mS m^{-1} . These initial values were maintained constant in all the experiment set-up. Thereupon, the obtained reject water was subjected to the Fe-EC reactor as mentioned in the following section.

2.2. Experimental set-up and procedure

The iron-electrocoagulation (Fe-EC) unit is schematized in Figure 1. It consisted of a cylindrical glass reactor (d : 9 cm, h : 12.5 cm) with an effective volume of 500 mL. To ensure a homogenous mixing during Fe-EC experiments, a magnetic stirrer (model SHA R-50, Iran) was placed at the bottom of the reactor at a constant rate of 250 rpm. Four iron electrodes (70 mm (width) \times 70 mm (length) \times 5 mm (depth)) were mounted on the EC reactor where the electrode gap was fixed at 10 mm. The electrodes were vertically placed in a monopolar-parallel connection using a power supply (model JPS303D Iran; E_{max} : 30 V) operated under galvanostatic mode. After each run, the electrodes were well polished with emery paper to avoid electrode passivation and then washed with acid reagent and distilled water to remove any impurities from the surface. All electrocoagulation runs were performed in triplicate showing a standard deviation below 3%; average data are reported.

The pH of the solution was monitored using a multi-parameter analyzer (CONSORT C831, Belgium). The pH value was maintained at approximately 8.0–8.5 by manual addition of 0.01 M H_2SO_4 and 0.1 M KOH to ensure minimum solubility of Cr(OH)_3 [3]. A digital calibrated conductivity meter (Leybold 666222, Germany) was used for electrical conductivity measurements.

At the end of each Fe-EC run, samples were collected and filtered through a 0.45- μm membrane filter for chromium analysis. The treated solution was allowed to settle for about 60 min in a quiescent state. The settled sludge volume values were recorded after complete settlement.

Collected samples were analysed for total chromium content by atomic absorption spectrophotometry using a BRAIC WFX-130 (China) spectrophotometer at 620 nm according to Standard Methods for the Examination of Water and Wastewater [23]. The chromium removal efficiency was calculated according to Equation (12) [22]:

$$R(\%) = \frac{C_0 - C_t}{C_0} \times 100 \quad (12)$$

where C_0 is the initial concentration of chromium and C_t is the effluent chromium concentration measured at the end of each electrocoagulation run in mg Cr L^{-1} .

The settled sludge volume (SSV) is one of the most important parameters for evaluating the performance of electrocoagulation. Sludge separation and dewatering is an essential part of coagulation-based treatment processes that can be costly. The settled sludge volume can be determined according to Equation (13):

$$\text{SSV (mL} \cdot \text{L}^{-1}) = \frac{A \times d}{V_s} \quad (13)$$

where A is the area of the cylindrical vessel (cm^2), d is the height occupied by the sludge (cm) and V_s is the total volume of water treated (L).

The operational cost (OPC), electrode material consumption (EMC) and electrical energy consumption (EEC) were the main parameters investigated in this case of study as techno-economic indicators for electrocoagulation competitiveness. These parameters were calculated according to the following equations [24–27]:

$$\text{OPC (USD} \cdot \text{m}^{-3}) = a \times \text{EMC} + b \times \text{EEC} \quad (14)$$

$$\text{EMC (kg} \cdot \text{m}^{-3}) = \frac{I \times t \times M}{z \times F \times V_s} \quad (15)$$

$$\text{EEC (kWh} \cdot \text{m}^{-3}) = \frac{E_{\text{cell}} I t}{1000 \times V_s} \quad (16)$$

where EMC and EEC present the consumption quantities of electrode material and electricity required for target

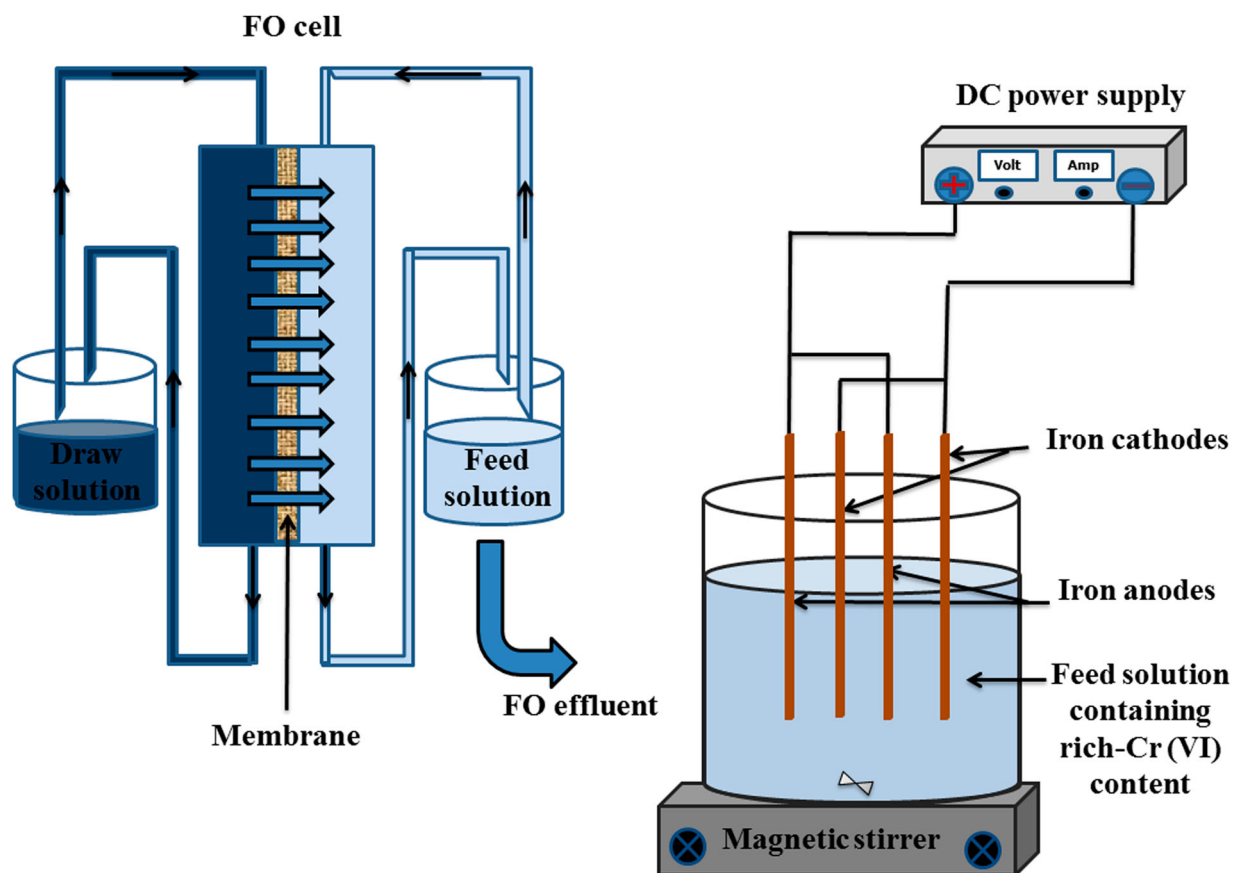


Figure 1. Fe-EC set-up for the removal of Cr(VI) from FOR in a monopolar-parallel connection (1 A; an applied current density (J) = 5.1 mA cm^{-2}).

pollutant removal. ' a ' ($\text{USD}\cdot\text{kW}\cdot\text{h}^{-1}$) and ' b ' ($\text{USD}\cdot\text{g}^{-1}$) are the price of electricity and electrode material, respectively. The variable I is the applied current (A), t is the electrolysis time (h), M is the molecular mass of iron (55.85 g mol^{-1}), z is the number of electrons transferred ($z = 2$), F is the Faraday's constant ($96,487 \text{ C mol}^{-1}$), V_s is the volume of the solution (m^3) and E_{cell} (V) is the average of the applied voltage in the cell.

2.3. Mathematical modelling for optimization

Traditionally, the most common practice in the study of operational parameters is the traditional single factor at time approach. It consists in looking for the effect of one factor, which must vary systematically, while keeping the other factors constant. The result of this univariate analysis does not guarantee the optimization of the parameters. This approach would only be valid if the factors to be optimized were totally independent of each other [28]. However, compared to single-factor and orthogonal experiments, where the optimization is found out through the study of multi-factor and level of design method by analysing each test point. Response

surface methodology (RSM) constructs an approximate model in the design space using known experimental data to that meets the fitting accuracy between the design variables and the target response [29]. Generally, RSM has the ability to model as many responses to measure, allows identifying the interactions between the independent variables, to model the system mathematically and to save time and money by reducing the number of experiments [30]. In this work, RSM was employed as the optimization tool through experimental design to maximize pollutant removal while minimizing operational expenditure. The analysis was depicted using expert design 10 software (Stat-Ease, Inc., Minneapolis, USA) to perform a full central composite design with five levels ($-1.68, -1, 0, +1, +1.68$), consisting of 13 points (8 experiments and 5 central points). The selected independent variables were electrocoagulation time (A: 15.09, 24, 45.50, 67 and 75.91 min) and current (B: 0.51, 0.8, 1.50, 2.20 and 2.49 A). The appropriate high and low ranges were defined according to some preliminary tests. The selected responses for process optimization were Cr(VI) removal efficiency, operating costs, electrical energy consumption and settled sludge volume.

The system was described by a numerical expression (Equation (17)) of the polynomial statistical model that allowed the mathematical description of the RSM [24,31]:

$$Y = \beta_0 + \sum_{i=1}^{i=k} \beta_i x_i + \sum_{i=1}^{i=k} \beta_{ii} x_i^2 + \sum_{1 \leq i < j} \beta_{ij} x_i x_j + \varepsilon \quad (17)$$

where Y represents the response and x_i and x_j are the coded independent variables. Then, β_0 is the constant coefficient of the model, β_i is the linear coefficient, β_{ii} is the quadratic effect coefficient, β_{ij} is the interaction effect coefficient and ε is the residual term associated with random error. Three replicates of the central point were conducted to estimate the pure error of experiments. The validation of the model was confirmed through analysis of variance (ANOVA) to ensure statistical significance.

For multi-response optimization, the desirability method is one of the most widely used approaches to respond to multi-objectives [32]. It associates an individual scale-free desirability (d_i), where $0 \leq d_i \leq 1$ [33] with each response (Y_i). The values d_i (0 and 1) present the complete refusal and maximum satisfaction of the response, respectively. The overall desirability (D) considers all response Y_i desirability and their requirements. D can be determined according to Equation (18) [9]:

$$D = \left[\prod_{i=1}^n d_i^{W_i} \right]^{\frac{1}{\sum W_i}} \quad (18)$$

where n and W_i represent the number of responses and the weighting factors of the response Y_i , respectively.

3. Results and discussions

3.1. Statistical analysis and model fitting via central composite design

Table 1 displays the experimental results of the central composite design matrix and the predicted responses from the fitted model for Cr(VI) removal by Fe-EC. The predicted values were close enough to those experimentally obtained, indicating good fitness. As shown in Table 1, a complete chromium removal was achieved at 13th electrocoagulation run operated at a current of 2.49 A ($J = 12.7 \text{ mA}\cdot\text{cm}^{-2}$) and an electrolysis time of 45.5 min. On contrary, the lowest current value (0.8 A) resulted in the cheapest operation cost (0.003 USD m^{-3}) together the lowest settled sludge volume (180 mL L^{-1}).

According to the obtained results, the central composite design under response surface methodology suggested a quadratic model. The quadratic equations for study responses considering coded factors were

obtained as follows:

$$\begin{aligned} \text{Cr(VI) removal efficiency(\%)} \\ = +90.69 + 1.97 \times A + 6.41 \times B - 1.36 \times A \\ \times B + 0.65 \times A^2 + 0.17 \times B^2 \end{aligned} \quad (19)$$

$$\begin{aligned} \text{OPC (USD)} = +0.013 + 6.578\text{E-}003 \times A \\ + 7.498\text{E-}003 \times B + 3.650\text{E-}003 \\ \times A \times B + 8.000\text{E-}005 \times A^2 \\ + 5.800\text{E-}004 \times B^2 \end{aligned} \quad (20)$$

$$\begin{aligned} \text{EEC (kWh}\cdot\text{m}^{-3}) = +5.233\text{E-}003 + 2.857\text{E-}003 \times A \\ + 4.157\text{E-}003 \times B \\ + 2.118\text{E-}003 \times A \times B \\ + 1.064\text{E-}004 \times A^2 \\ + 8.000\text{E-}004 \times B^2 \end{aligned} \quad (21)$$

$$\begin{aligned} \text{SSV (mL}\cdot\text{L}^{-1}) = +499.00 + 91.11 \times A + 247.71 \\ \times B + 50.00 \times A \times B - 17.94 \\ \times A^2 - 6.69 \times B^2 \end{aligned} \quad (22)$$

where A and B are the coded terms for the independent variables of the chosen response as mentioned in Table 1.

The ANOVA results are outlined in Table S1. As can be seen, all terms in the statistical quadratic model were highly significant ($p < 0.0001$). Meanwhile, F -values for Cr(VI) removal of 127.68, operating cost of 982.04, electrical energy consumption of 139.55 and settled sludge volume of 183.44 were non-significant, which implied that there were only 0.01% chance that the F -values were out of design due to noise. Accordingly, good fits to the quadratic model were confirmed by large F -values, small p -values, and large values of R^2 , R^2 adjusted, and R^2 predicted.

Based on the ANOVA results, Adeq precision (AP) measures the signal-to-noise ratio, in other words, a measure of predicted response value range at the design points relative to associated mean prediction error. A ratio greater than 4 is desirable. AP values of 35.417, 99.506, 37.035 and 42.992 for Cr removal, operating cost, electrical energy consumption and settled sludge volume, respectively, indicated an adequate signal and high capability of developed models in predicting the results. Coefficient of variance (CV) describes the precision and reproducibility of a model. A model with a ratio less than 10% is considered reproducible. CV values of acceptable ranges from 0.83 to 9.83% proved the reproducibility of the model and high precision of obtained results. The lack-of-fit test (LOF test) describes the variation of data around the fitted

Table 1. Design matrix of experiments and results of CCD.

| Run | Std | Experimental matrix | | Responses | | | | | | | |
|-----|-----|---------------------|-------|----------------|-----------|----------------------------|-----------|----------------------------|-----------|---------------------------|-----------|
| | | | | Cr removal (%) | | OPC (USD·m ⁻³) | | EEC (kWh·m ⁻³) | | SSV (mL·L ⁻¹) | |
| | | A | B | Actual | Predicted | Actual | Predicted | Actual | Predicted | Actual | Predicted |
| 1 | 3 | -1 | +1 | 97.9 | 97.3 | 0.011 | 0.011 | 0.005 | 0.005 | 590 | 580 |
| 2 | 4 | +1 | +1 | 98.4 | 98.6 | 0.031 | 0.031 | 0.015 | 0.015 | 860 | 863 |
| 3 | 11 | 0 | 0 | 90.6 | 90.7 | 0.013 | 0.013 | 0.006 | 0.005 | 495 | 499 |
| 4 | 6 | +1.68 | 0 | 94.9 | 94.8 | 0.022 | 0.022 | 0.009 | 0.009 | 605 | 591 |
| 5 | 5 | -1.68 | 0 | 88.3 | 89.2 | 0.004 | 0.004 | 0.002 | 0.001 | 330 | 334 |
| 6 | 9 | 0 | 0 | 91.3 | 90.7 | 0.013 | 0.012 | 0.006 | 0.005 | 535 | 499 |
| 7 | 10 | 0 | 0 | 91.0 | 90.7 | 0.013 | 0.013 | 0.006 | 0.005 | 520 | 499 |
| 8 | 7 | 0 | -1.68 | 81.9 | 82 | 0.004 | 0.003 | 0.001 | 0.001 | 150 | 135 |
| 9 | 13 | 0 | 0 | 89.9 | 90.7 | 0.012 | 0.013 | 0.004 | 0.005 | 485 | 499 |
| 10 | 12 | 0 | 0 | 90.1 | 90.3 | 0.013 | 0.012 | 0.005 | 0.005 | 460 | 499 |
| 11 | 2 | +1 | -1 | 88.7 | 88.4 | 0.009 | 0.009 | 0.003 | 0.003 | 250 | 267 |
| 12 | 1 | -1 | -1 | 82.8 | 81.8 | 0.003 | 0.003 | 0.001 | 0.001 | 180 | 185 |
| 13 | 8 | 0 | +1.68 | 100 | 100.1 | 0.025 | 0.025 | 0.013 | 0.013 | 830 | 835 |

model. The LOF test would be non-significant if the model fits the data well. The LOF test for Cr(VI) removal ($p = 0.1331$), operating cost ($p = 0.9253$), electrical energy consumption ($p = 0.9351$) and settled sludge volume ($p = 0.8008$) were not statistically significant, reinforcing that those points were properly distributed around the fitted model.

The diagnostics of the experimental data yielded the graphical results given in Figures 2 and 3. Four aspects of graphical model validation are (i) the normal probability plot of residuals (Figure 2(a-d)); (ii) externally studentized residuals vs. predicted (Figure 2(e-h)); (iii) externally studentized residuals vs. run number (Figure 3(a-d)) and (iv) predicted vs. actual plots (Figure 3(e-h)). The residuals almost lied on or close to the normal probability line (Figure 2(e-h)), which indicated the presence of very minimal errors in experimentation and testified the reliability of the quadratic model. Moreover, as is visible in Figure 3(a-d), the residuals lied well within the acceptable range from -3 to $+3$ which further validated the quadratic model. The actual vs. predicted plots displayed that the experimental data approximately overlapped with the predicted data (Figure 3(e-h)), contributing as the last nail in the coffin of model.

3.2. Interaction of electrolysis time and applied current on chromium removal

In the EC process, the amount of electro-dissolved iron ions generated by the anode depends on the current and electrolysis time in accordance with Faraday's Law (Equation (15)). An increase in the current density (J ; mA cm⁻²) or the current (I ; A) accelerates the reaction rate due to an increase in the amount of iron dissolved at cathode [34–36]. At pH values between 7.5 and 8.1, this increase in the Cr(IV) reduction rate was explained by an increase in concentrations of FeOH⁺ and Fe(OH)₂⁰ [37,38]. Increasing current or prolonging electrolysis

time also induces the formation of OH⁻ ions owing to the water reduction reaction occurring at the cathode (Equation (2)), resulting in the precipitation of amorphous Fe(OH)₃ solid [39]. At slightly alkaline pH, Cr(III) ions are combined with OH⁻ ions to produce insoluble Cr(OH)₃ in the bulk solution [21,39,40]. Furthermore, two Cr(VI) removal mechanisms were proposed by Heidmann and Calmano [35] depending on the current value for the EC process utilizing iron electrodes. According to their approach, at high currents varying between 1.0 and 3.0 A, Cr(VI) might be directly reduced to Cr(III) at the cathode surface prior to precipitation as Cr(OH)₃. At low currents from 0.05 to 0.1 A, Fe(II) produced by the dissolution of iron anodes worked as a reducing agent to reduce Cr(VI) to Cr(III) before precipitating as Cr(OH)₃ together with either Fe(OH)₂ or Fe(OH)₃ depending on the formation of oxygen at the cathode [35]. As mentioned in the following subsection, in our case, the second seems to be responsible for the chromium removal mechanism even at high currents.

Both experimental and model data obtained in the present study are consistent with the relevant literature [34,38]. As can be seen in Table 1, chromium removal efficiency significantly improved with increasing current, and a complete chromium removal was achieved at the highest applied current (2.49 A; $J = 12.7$ mA cm⁻²). Similarly, an extension in electrocoagulation treatment time had an enhancement effect on process performance in terms of chromium removal for the current up to 2.2 A ($J = 11.22$ mA cm⁻²). Together with this observation, it is worth noting that an extending electrolysis time from 24 to 67 min resulted in only 0.5% additional chromium removal (cf. runs 1 and 2) for a current value of 2.2 A.

Figure 4(a-b) emphasizes the mutual interaction between current and electrolysis time. Data indicated that almost complete chromium removal could be obtained by arranging of either current or electrolysis

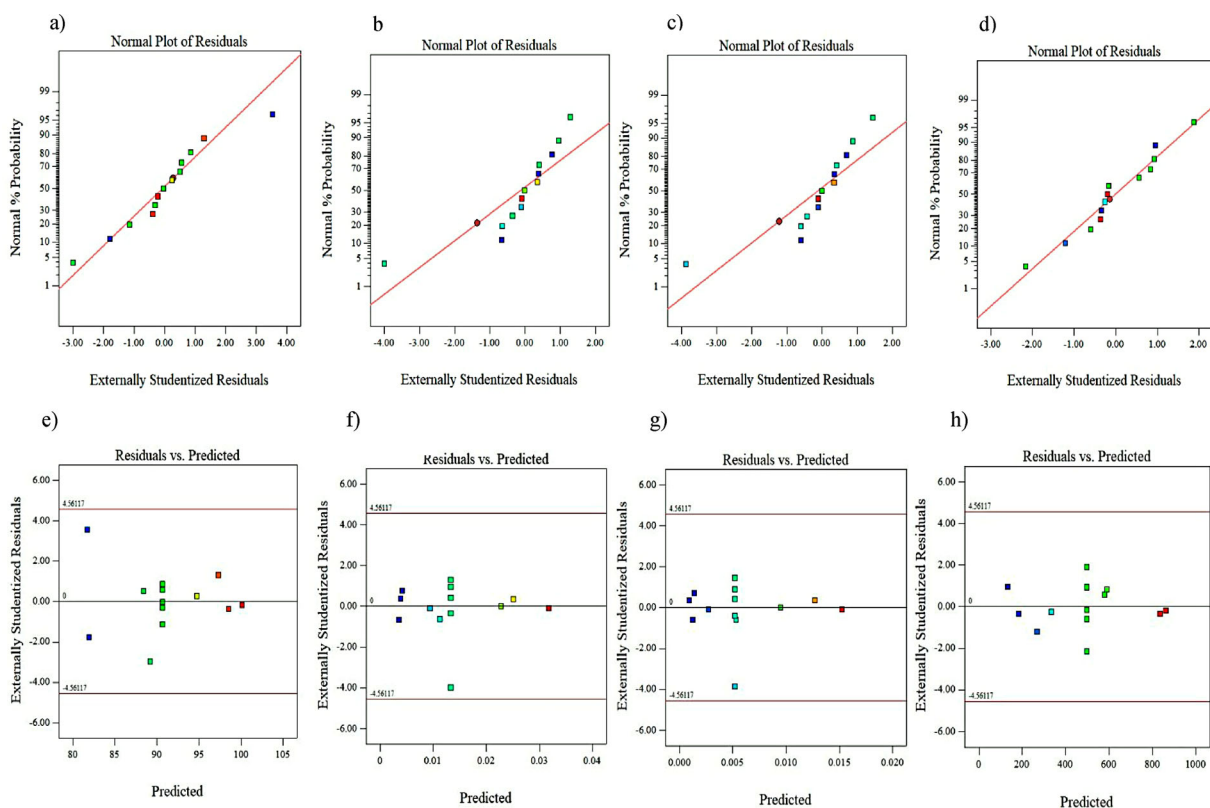


Figure 2. Validation of the model. Normal plot of residuals: (a) Cr removal, (b) operating cost, (c) electrical energy consumption and (d) settled sludge volume. Residuals vs predicted: (e) Cr removal, (f) operating cost, (g) electrical energy consumption and (h) settled sludge volume.

time as (i) increasing the current from 0.5 ($J = 2.55 \text{ mA cm}^{-2}$) to 2.49 A ($J = 12.7 \text{ mA cm}^{-2}$) (100%) for an electrolysis time of 45 min or (ii) extending electrocoagulation treatment time to 69 min (98.4%) at a current value of 2.2 A ($J = 11.22 \text{ mA cm}^{-2}$).

In the present study, where the initial Cr(VI) concentration was 69 mg L^{-1} , the optimum operation conditions were determined as an electrolysis time of 59.7 min and a current of 1.24 A ($J = 6.32 \text{ mA cm}^{-2}$). About 89.7% chromium removal was attained at these conditions. This efficiency is similar with that obtained by Deveci et al. [41]. They achieved a 86.27% Cr(VI) removal at electrocoagulation conditions: current of 0.675 A, initial pH of 8, an electrolysis time of 60 min, and a conductivity of 56.2 mS cm^{-1} at $20^\circ\text{C} (\pm 0.1)$ for a raw tannery wastewater (Cr(VI): 22.3 mg L^{-1} and COD: $18,800 \text{ mg L}^{-1}$). Borba et al. [42] studied the chromium removal from real tannery wastewater. The authors reported a 96.2% of removal efficiency using the following optimal parameters: pH 4, current density of 68.4 mA cm^{-2} and electrolysis time of 120 min. Khan et al. [36] reported that (i) process removal efficiency was more sensitive to the applied current and (ii) complete chromium (Cr(IV) of 49.96 mg L^{-1}) removal could be achieved at optimum

conditions: an applied current of 1.48 A, pH of 3.0 and an electrolysis time of 21.47 min. Gong et al. [43] obtained conflicting results in the treatment of reverse osmosis concentrates from petrochemical wastewater by the Fe-EC process, which found that less than 20% of chromium was removed within 20 min at 30 mA cm^{-2} . This difference may be due to the fact that with increasing EC time, the pH changes which directly affect the formation of Fe(III) hydroxides and Fe(II) hydroxides during the Fe-EC process that finally affects the Cr(IV) removal [44].

3.3. Interaction of electrolysis time and current on settled sludge volume

Figure 5(a,b) exhibits the settling behaviour of flocs as a function of EC time and current value. All SSV analyses were evaluated for 60 min settling period. This means that after stopping the stirring, we allow the flocs to settle for 60 min. As expected, increasing current as well as EC time induced an increase in the sludge production due to increase in the co-precipitation of iron hydroxides with $\text{Cr}(\text{OH})_3$. Depending on effluent pH reached at the end of EC operation, $\text{Cr}(\text{OH})_3$ may co-precipitate together with $\text{Fe}(\text{OH})_3$ flocs as aforementioned.

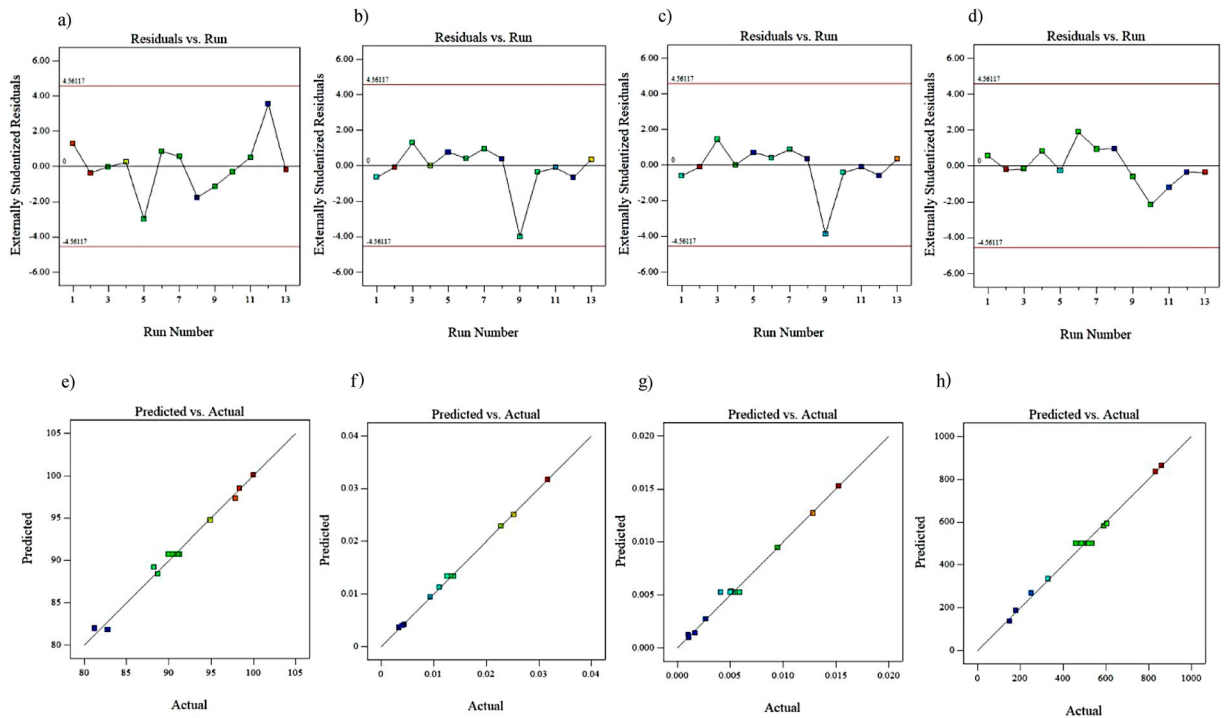


Figure 3. Validation of the model. Residuals vs run: (a) Cr removal, (b) operating cost, (c) electrical energy consumption and (d) settled sludge volume. Predicted vs actual plots: (e) Cr removal, (f) operating cost, (g) electrical energy consumption and (h) settled sludge volume.

In our case, because solution pH was kept at a range of 8.0–8.5, both solid phases assumed to be generated during EC treatment, resulting in high SSV values particularly at increasing currents. The formation of two solids at pH greater than 7.0 was also confirmed by literature data [36,38].

The flocs produced at the highest current value were the most difficult to settle, particularly, for current value of 2 A ($J = 10.2 \text{ mA cm}^{-2}$). For instance, elevating current from 0.8 to 2.2 A ($J = 4.08\text{--}11.22 \text{ mA cm}^{-2}$), high SSV corresponding to 180 and 590 mL L^{-1} within 24 min of Fe-EC were produced. A similar trend was observed for all

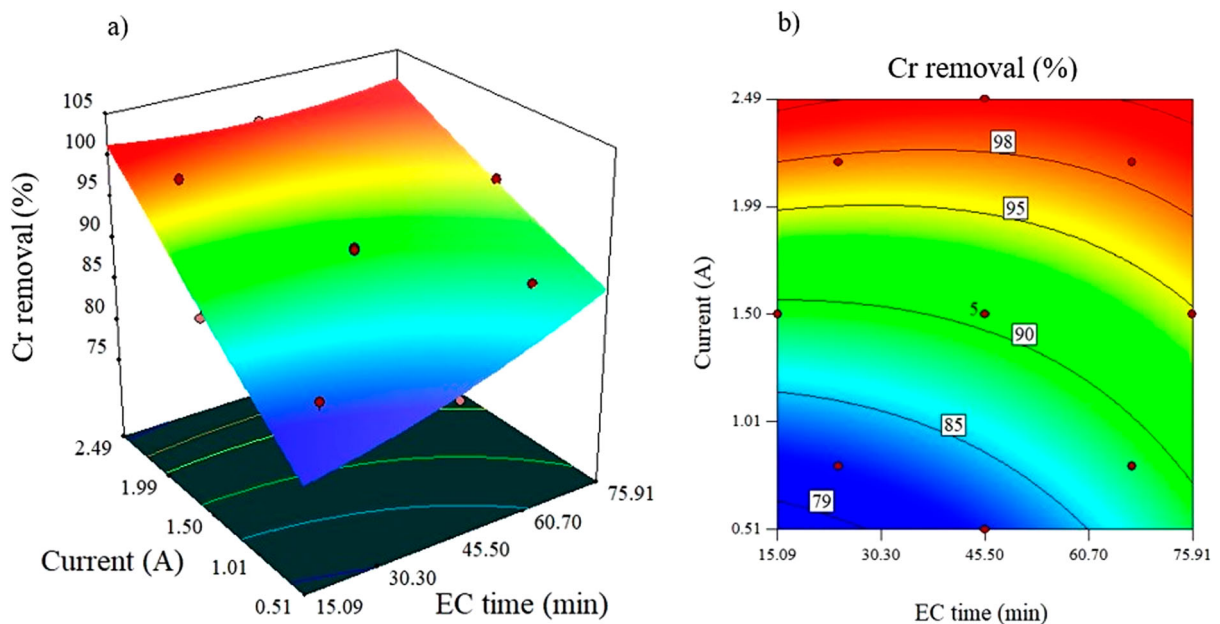


Figure 4. (a) 3D plot and (b) 2D contours for chromium removal: effect of current and electrolysis time.

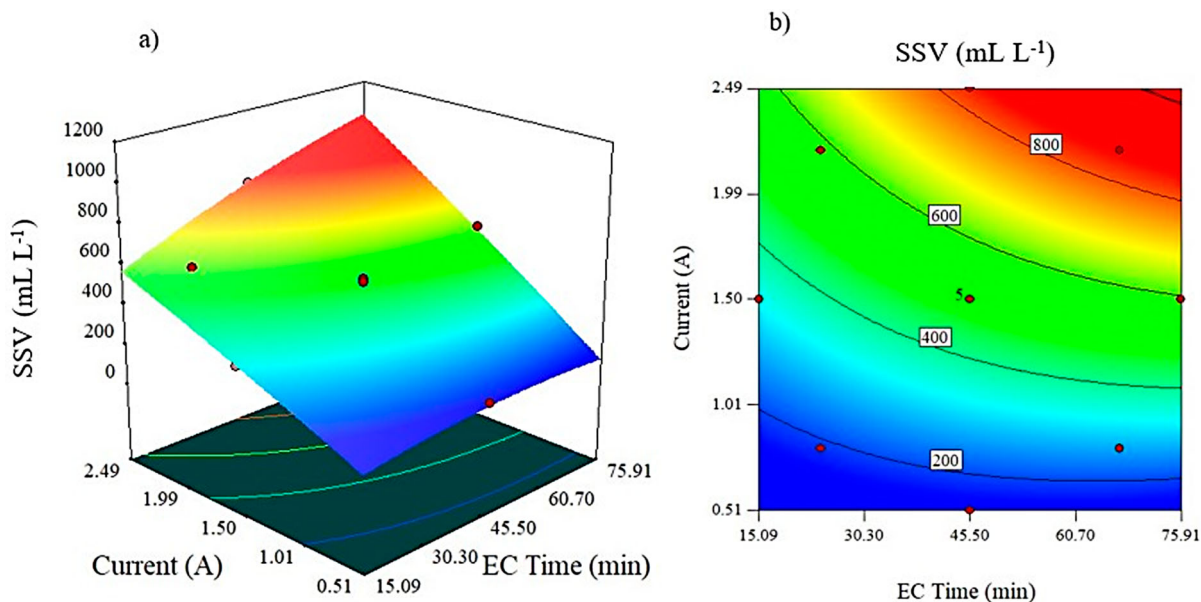


Figure 5. (a) 3D plot and (b) 2D contours for settled sludge volume: effect of current and electrolysis time.

Fe-EC runs with different operating times. The SSV values ranged between 495 and 830 mL L⁻¹ for Fe-EC performed during 45.5 min or longer. High SSV values were obtained at extended EC times or higher current intensities. Ölmez [38] experimentally treated the chromium plating process (Cr(VI): 1470 mg L⁻¹) by EC with stainless steel electrodes. In that study, SSV was obtained as 928 mL L⁻¹ (sludge volume index = 80 mL g⁻¹, sludge = 11.6 g VSS·L⁻¹) at optimum EC conditions: a current value of 7.4 A, an EC time of 70 min and an initial pH of 11.0. It is obvious that during Fe-EC, hydrogen bubbles are evolved at the cathode and can be trapped in the flocs consequently provoking them to float [45]. As a result, the lower the current value of the FOR in the Fe-EC cell, the more bubbles formed and the more likely flotation occurring. As shown in Figure 5(a,b), this phenomenon was most notable when the current value was lower than 1.5 A ($J = 7.65 \text{ mA cm}^{-2}$) at the initial EC time (30 min).

In general, the SSV data was in line with the results of Brahmi et al. [46] showing that the most important drawback of the EC process are the long settling time periods. Whilst the results were contrary to the opinion of Ashraf et al. [47] who found that over time, the flocs settled well and reached a minimum of about 200 mL L⁻¹.

3.4. Interaction of electrocoagulation time and current on electrical energy consumption

Electrical energy consumption is defined as the amount of electrical energy consumed per unit volume (m³) of wastewater to be treated. Electrical energy consumption

together with electrode material consumption are generally used to estimate the operating cost of EC. Therefore, the effect of current and EC time on electrical energy consumption were explored at a range of 0.5–2.5 A ($J = 2.55\text{--}12.75 \text{ mA cm}^{-2}$) and 15–76 min, respectively. Figure 6 depicts (a) 3D plots and (b) 2D counters as a function of current and EC time on electrical energy consumption.

Extending Fe-EC operation time significantly increased the electrical energy consumption as well as improved process efficiency at all tested conditions. For instance, an extension in EC time from 24 to 67 min resulted in a threefold increase in electrical energy consumption in both current values of 0.8 and 2.2 A ($J = 4.08\text{--}11.22 \text{ mA cm}^{-2}$). It is obvious that the effect of EC time on electrical energy consumption became significant when the current increased. The highest electrical energy consumption was determined as 0.015 kWh m⁻³ at a current value of 2.2 A ($J = 11.22 \text{ mA cm}^{-2}$) and at an EC time of 67 min. For an EC time of 45.5 min, current values of 0.5, 1.5 and 2.49 A ($J = 2.55, 7.65 \text{ and } 12.7 \text{ mA cm}^{-2}$) yielded electrical energy consumptions of 0.001, 0.005 and 0.013 kWh m⁻³, respectively, indicating that this operating parameter also has a significant effect on electrical energy consumption. In these Fe-EC experiments, complete Cr(VI) removals were achieved. These findings were in good agreement with the recent literature [36,48–51] which reported that values of specific energy consumption were directly proportional to the applied current and inversely proportional to the amount of Cr(VI) removed.

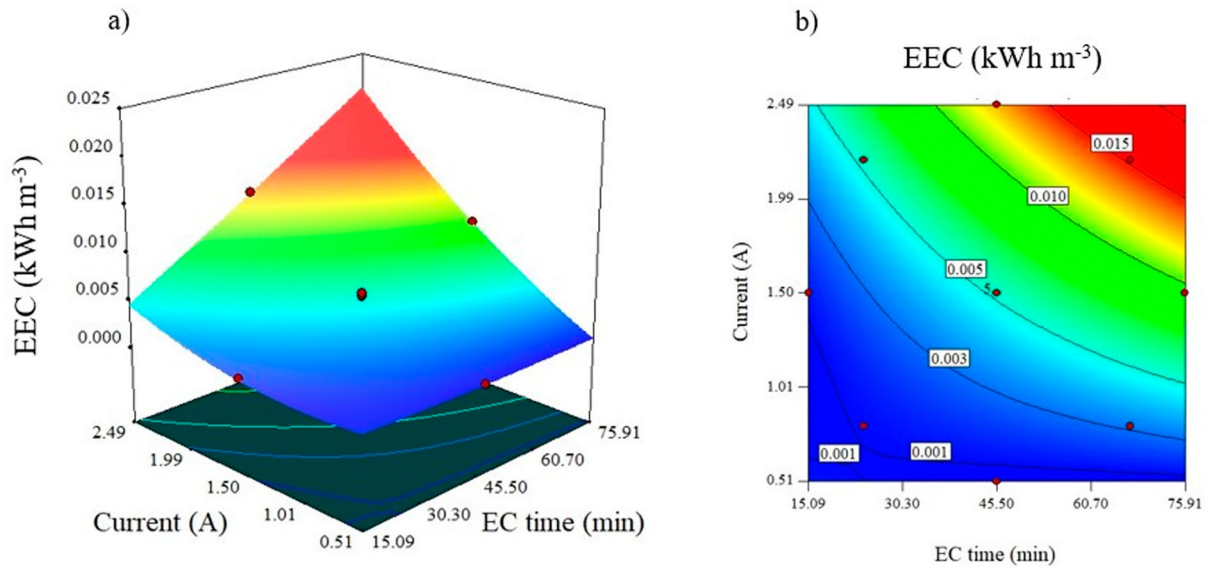


Figure 6. (a) 3D plot and (b) 2D contours for electrical energy consumption: effect of current and electrolysis time.

3.5. Interaction of electrolysis time and current on operating cost

As given in Equation (16), the operating cost incurred in Fe-EC are associated with electrode and energy consumptions. Both consumptions are strictly dependent on cell voltage, current and EC time. An extended EC may cause the passivation of the working electrodes and subsequently high cell potentials would be required. These higher values will increase energy consumption and costs. However, the FOR used in this work showed high electrical conductivity (18 mS cm⁻¹). This last avoided the formation of this passive film.

Figure 7 exhibits the combined effect of EC time and applied current on operating cost. The cost of the Fe-EC, when a complete abatement of chromium was achieved was 0.025 USD m⁻³ (0.013 kWh m⁻³). However, as mentioned above, the current and the EC time influenced these operating costs. For instance, a quasi-complete reduction in Cr(VI) concentrations (98.3% and 97.9%) observed operation costs of 0.031 USD m⁻³ (0.015 kWh m⁻³) and 0.011 USD m⁻³ (0.005 kWh m⁻³). These last values strongly depended on the reaction time. In the same venue, poor removal efficiency (81.2%) was observed at 0.51 A ($J = 2.6 \text{ mA}\cdot\text{cm}^{-2}$) and

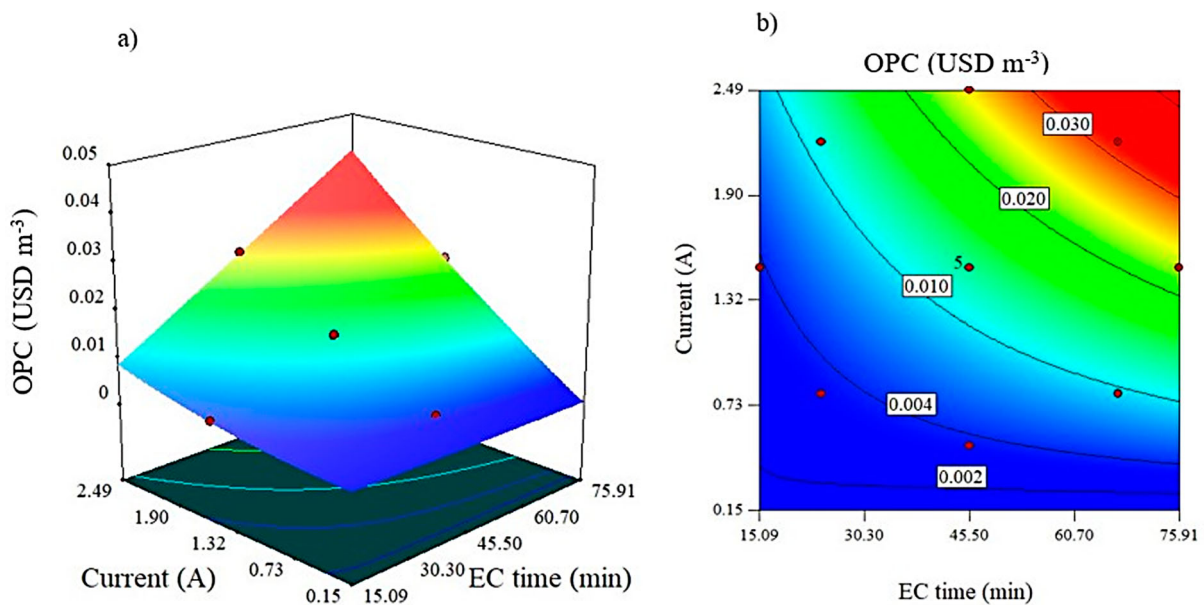


Figure 7. (a) 3D plot and (b) 2D contours for operating cost: effect of current and electrolysis time.

Table 2. Comparison with the literature data.

| Electrodes | Operating parameters | Cr(VI) removal | Energy consumption | Operating costs | Reference |
|------------|---|----------------|---|--------------------------------------|----------------------------|
| Fe | pH 3.0, 1.48 A, 21.47 min | 100% | 12.97 Wh.(g Cr ^a) ⁻¹ | – | [36] |
| Al | Al-AlAl-Al, 11.57 A·m ⁻² , electrode gap 1 cm | 77.6%–97.9% | – | 3.148USD·m ⁻³ | [57] |
| Fe | 20 mA·cm ⁻² , pH 2.4, 0.05 M NaCl electrolyte, Cr(VI) ₀ = 1000 mg·L ⁻¹ | 100% | 2.68 kWh·m ⁻³ | – | [20] |
| Fe + Al | pH 9, t = 20 min | 100% | 0.37–2.78 kWh·m ⁻³ | – | [58] |
| Al | 6 mA·cm ⁻² 100 rpm | | 1.98 kWh·m ⁻³ | 0.7 USD m ⁻³ ^b | [40] |
| Fe | 6.32 mA·cm ⁻² ; 59.7 min | 89.7% | 0.008 kWh·m ⁻³ | 0.017 USD·m ⁻³ | Present study ^c |

^aThe removed Cr(VI); ^bproduced aluminium; ^cexperimental study results.

45.5 min of current and EC time, respectively. These last conditions produced an Fe-EC treatment cost of 0.004 USD m⁻³ (0.001 kWh m⁻³). In this regard, both the percentage of pollutant removal and the operating costs must be assessed to consider the optimal operating conditions. In these experiments, the cell voltage varied from 2.9 to 3.4 V. Bhatti et al. [52] reported the energy consumption as 137.2 kWh m⁻³ to achieve a 90.4% of chromium removal efficiency for an electrocoagulation operated at pH of 5, a current of 24 V, and 24 min treatment time. In the same vein, Khan et al. [36] reported that energy consumption (12.97 kWh g⁻¹) for a complete removal of Cr(VI) was reduced when solutions with higher initial concentration were treated at lower applied current for longer durations. Elabbas et al. [53] stated that the efficient treatment to remove chromium by electrocoagulation (using aluminium electrodes) required around 20 kWh m⁻³ (initial concentration 7000 mg L⁻¹). Oden and Sari-Erkan [54] calculated the operational cost of electrocoagulation for a complete chromium removal from a metal plating wastewater as 5.34 USD m⁻³. Additional literature for hexavalent chromium removal by EC utilizing either aluminium (Al) or iron (Fe) electrodes are also given in Table 2.

Electrical energy consumption revealed an exponential increase with applied current at the same EC time (45 min). These last two variables had a synergistic effect on the operating costs in terms of energy consumption. However, additional experiments using different electrode material, inter-electrode gap, as well as the mode of operation would be needed to enhance chromium removal efficiency in terms of energy consumption. Finally, it is important to note that the operating costs may fluctuate based on the geographical area and domestic values.

3.6. Desirability function, optimization and cost-effectiveness estimation

The desirability function aims to find the optimized conditions that satisfy multi-objective responses, with values between 0 and 1, where 0 represents an

undesirable value and 1 a desirable value [55]. In the present study, the desirability function was used to maximize chromium removal efficiency while minimizing electrical energy consumption, operating cost and settled sludge volume. Same importance was attributed to each response (weighting factor 1). The optimum conditions for Fe-EC were predicted by the response surface methodology and central composite design model as an EC time of 59.7 min and a current of 1.24 A ($J = 6.32 \text{ mA cm}^{-2}$). As per the model predictions, Cr(VI) removal efficiency, operating cost, electrical energy consumption and settled sludge volume were calculated as 90%, 0.014 USD m⁻³, 0.005 kWh m⁻³ and 445 mL L⁻¹, respectively. To control the applicability of the optimum conditions, an affirmative Fe-EC experiment was performed. The experimental results demonstrated Cr(VI) removal of 89.7%, operating cost of 0.017 USD m⁻³, electrical energy consumption of 0.008 kWh m⁻³ and settled sludge volume of 515 mL L⁻¹ were attainable under such optimum conditions. These results agreed with the predicted values, suggesting the appropriateness and accuracy of these optimization tools. However, even when lower EC costs were estimated, renewable energy-driven electrochemical technologies from laboratory to industrial scale is a crucial issue in commercialization scope as well as in the autonomy of the process. In this way, on-grid solar photovoltaic energy could benefit the scale-up and industrialization of the electrochemical technology, as already is studied by other research groups [17, 56].

4. Conclusion

In the present study, Fe-EC/filtration/sedimentation proved to be an efficient and promising Cr(VI) removal method for the FOR. The following conclusions could be drawn from the present study:

- Complete Cr(VI) removal could be achieved at a current density of 16.94 mA cm⁻² and an EC time of 45.5 min. However, the lowest current density

(5.44 mA cm⁻²) resulted in the cheapest operation cost (0.003 USD m⁻³) together the lowest SSV (180 mL L⁻¹) as well as 82.8% Cr(VI) removal percentage.

- The optimal predicted conditions of the response surface methodology and central composite design based on the highest Cr(VI) removal while minimizing operation cost and SSV were an EC time of 59.7 min and a current density of 6.32 mA cm⁻². According to optimization, satisfactory performance was achieved for Cr(VI) removal efficiency, electrical energy consumption, OC, and SSV of 90%, 0.005 kWh m⁻³, 0.014 USD m⁻³, and 445 mL L⁻¹, respectively. This prediction agreed with the experimental results (89.7%, 0.008 kWh m⁻³, 0.017 USD m⁻³, and 515 mL L⁻¹, respectively).
- Although FO has proved its potential in wastewater treatment, the integration of other treatment technologies such as EC as a post-treatment can diminish substantially the volume of reject water and maximize water reuse. In addition, treatment and regeneration of FOR would be economically feasible. In this sense, a research into renewable and cleaner energy sources to efficient energy management practices and optimize resource utilization must be emphasized.
- In future research, the reduction kinetics analysis which indicates the reduction behaviour and the reduction mechanism of Cr(VI) via electrochemical process will be discussed. Beyond that, a new kinetic model will be developed to simulate for the reduction behaviour of Cr(VI) under both isothermal and non-isothermal conditions.

Disclosure statement

No potential conflict of interest was reported by the author(s).





Funding

The support of the Research Vice-Chancellor of Qazvin University of Medical Sciences is wholeheartedly appreciated (IR.QUMS.REC.1400.122). Milad Mousazadeh is thankful to the Iran's National Elites Foundation (INEF) for granting the Elite Award, No. 15/11529. Miguel Angel Sandoval is grateful to Agencia Nacional de Investigación y Desarrollo (ANID-FONDECYT, Chile) for granting the postdoctoral scholarship, No. 3200274.

Data availability statement

The authors confirm that the data supporting the findings of this study are available within the article.

ORCID

Milad Mousazadeh  <http://orcid.org/0000-0003-1464-3915>
Fatima Ezzahra Titchou  <http://orcid.org/0000-0002-0515-2295>
Mahmoud Nasr  <http://orcid.org/0000-0001-5115-135X>
Mohammad Mahdi Emamjomeh  <http://orcid.org/0000-0003-2772-6832>

References

- [1] Perraki M, Vasileiou E, Bartzas G. Tracing the origin of chromium in groundwater: current and new perspectives. *Curr Opin Environ Sci Health*. 2021; 22:100267.
- [2] Tünay O, Kabdaşlı I, Arslan-Alaton I, et al. Chemical oxidation applications for industrial wastewaters 1st ed. London: IWA Publisher; 2010.
- [3] Tünay O, Kabdaşlı I, Hung Y-T. Treatment of metal finishing wastes. In: Wang LK, Hung Y-T, Lo HH, Yapijakis C, editor. *Handbook of industrial hazardous waste treatment*. Boca Raton: Marcel Dekker Inc.; 2007. p. 289–359.
- [4] Karimi-Maleh H, Orooji Y, Ayati A, et al. Recent advances in removal techniques of Cr (VI) toxic ion from aqueous solution: a comprehensive review. *J Mol Liq*. 2021;329:115062.
- [5] Palmer CD, Puls RW. Natural attenuation of hexavalent chromium in groundwater and soils. 1994. https://www.epa.gov/sites/default/files/2015-06/documents/natatt_hexavalent_chromium.pdf
- [6] WHO. Guidelines for drinking-water quality: volume 1: recommendations, 2nd ed. World Health Organization. 1993. <https://apps.who.int/iris/handle/10665/259956>
- [7] EPA. Chromium in drinking water. United States Environmental Protection Agency. Accessed May 5, 2021. <https://www.epa.gov/sdwa/chromium-drinking-water>.
- [8] GracePavithra K, Jaikumar V, Kumar PS, et al. A review on cleaner strategies for chromium industrial wastewater: present research and future perspective. *J Cleaner Prod*. 2019;228:580–593.
- [9] Kerur S, Bandekar S, Hanagadakar MS, et al. Removal of hexavalent Chromium-Industry treated water and Wastewater: a review. *Materials Today: Proceedings*. 2021.
- [10] Prasad S, Yadav KK, Kumar S, et al. Chromium contamination and effect on environmental health and its remediation: a sustainable approaches. *J Environ Manag*. 2021;285:112174.
- [11] Ang WL, Mohammad AW, Johnson D, et al. Forward osmosis research trends in desalination and wastewater treatment: a review of research trends over the past decade. *J Water Process Eng*. 2019;31:100886.
- [12] Chia WY, Chia SR, Khoo KS, et al. Sustainable membrane technology for resource recovery from wastewater: forward osmosis and pressure retarded osmosis. *J Water Process Eng*. 2020: 101758.
- [13] Coday BD, Xu P, Beaudry EG, et al. The sweet spot of forward osmosis: treatment of produced water, drilling wastewater, and other complex and difficult liquid streams. *Desalination*. 2014;333:23–35.
- [14] Singh SK, Sharma C, Maiti A. A comprehensive review of standalone and hybrid forward osmosis for water

- treatment: membranes and recovery strategies of draw solutions. *J Environ Chem Eng.* **2021**;9:105473.
- [15] Ibrar I, Altaee A, Zhou JL, et al. Challenges and potentials of forward osmosis process in the treatment of wastewater. *Crit Rev Environ Sci Technol.* **2020**;50:1339–1383.
- [16] Ezugbe E O, Rathilal S. Membrane technologies in wastewater treatment: a review. *Membranes.* **2020**;10:89.
- [17] Garcia-Segura S, Eiband MMS, de Melo JV, et al. Electrocoagulation and advanced electrocoagulation processes: a general review about the fundamentals, emerging applications and its association with other technologies. *J Electroanal Chem.* **2017**;801:267–299.
- [18] Sandoval MA, Fuentes R, Thiam A, et al. Arsenic and fluoride removal by electrocoagulation process: a general review. *Sci Total Environ.* **2021**;753:142108.
- [19] Aoudj S, Khelifa A, Drouiche N, et al. Simultaneous removal of chromium(VI) and fluoride by electrocoagulation–electroflotation: application of a hybrid Fe–Al anode. *Chem Eng J.* **2015**;267:153–162.
- [20] Un UT, Onpeker SE, Ozel E. The treatment of chromium containing wastewater using electrocoagulation and the production of ceramic pigments from the resulting sludge. *J Environ Manag.* **2017**;200:196–203.
- [21] Mouedhen G, Feki M, De Petris-Wery M, et al. Electrochemical removal of Cr(VI) from aqueous media using iron and aluminum as electrode materials: towards a better understanding of the involved phenomena. *J Hazard Mater.* **2009**;168:983–991.
- [22] Naghdali Z, Sahebi S, Mousazadeh M, et al. Optimization of the forward osmosis process using aquaporin membranes in chromium removal. *Chem Eng Technol.* **2020**;43:298–306.
- [23] APHA. Standard methods for the examination of water and wastewater. Washington, DC, USA: American Public Health Association (APHA); **2005**.
- [24] Mousazadeh M, Alizadeh S, Frontistis Z, et al. Electrocoagulation as a promising defluoridation technology from water: a review of state of the Art of removal mechanisms and performance trends. *Water (Basel).* **2021**;13:656.
- [25] Niazmand R, Jahani M, Sabbagh F, et al. Optimization of electrocoagulation conditions for the purification of table olive debittering wastewater using response surface methodology. *Water (Basel).* **2020**;12:1687.
- [26] Titchou FE, Afanga H, Zazou H, et al. Batch elimination of cationic dye from aqueous solution by electrocoagulation process. *Mediterr J Chem.* **2020**;10:1–12.
- [27] Titchou FE, Zazou H, Afanga H, et al. Removal of persistent organic pollutants (POPs) from water and wastewater by adsorption and electrocoagulation process. *Ground Sustain Dev.* **2021**;13:100575.
- [28] Geiger EO. Statistical methods for fermentation optimization. *fermentation and biochemical engineering handbook.* Elsevier; **1996**. p. 161–180.
- [29] Yang M, Gan Y, Gao L, et al. A structural optimization model of a biochemical detection micromixer based on RSM and MOEA/D. *Chem Eng Proces - Process Intensif.* **2022**;173:108832.
- [30] Toor UA, Duong TT, Ko S-Y, et al. Optimization of Fenton process for removing TOC and color from swine wastewater using response surface method (RSM). *J Environ Manag.* **2021**;279:111625.
- [31] Emamjomeh MM, Mousazadeh M, Mokhtari N, et al. Simultaneous removal of phenol and linear alkylbenzene sulfonate from automotive service station wastewater: optimization of coupled electrochemical and physical processes. *Sep Sci Technol.* **2020**;55:3184–3194.
- [32] Asante-Sackey D, Rathilal S, Pillay L V, et al. Ion exchange dialysis for aluminium transport through a face-centred central composite design approach. *Processes.* **2020**;8:160.
- [33] Ano J, Briton BGH, Kouassi KE, et al. Nitrate removal by electrocoagulation process using experimental design methodology: a techno-economic optimization. *J Environ Chem Eng.* **2020**;8:104292.
- [34] Zhou R, Liu FY, Wei N, et al. Comparison of Cr(VI) removal by direct and pulse current electrocoagulation: implications for energy consumption optimization, sludge reduction and floc magnetism. *J Water Process Eng.* **2020**;37:101387.
- [35] Heidmann I, Calmano W. Removal of Cr(VI) from model wastewaters by electrocoagulation with Fe electrodes. *Sep Purif Technol.* **2008**;6:15–21.
- [36] Khan SU, Islam DT, Farooqi IH, et al. Hexavalent chromium removal in an electrocoagulation column reactor: process optimization using CCD, adsorption kinetics and pH modulated sludge formation. *Process Saf Environ Prot.* **2019**;122:118–130.
- [37] Sedlak DL, Chan PG. Reduction of hexavalent chromium by ferrous iron. *Geochim Cosmochim Acta.* **1997**;61:2185–2192.
- [38] Olmez T. The optimization of Cr(VI) reduction and removal by electrocoagulation using response surface methodology. *J Hazard Mater.* **2009**;162:1371–1378.
- [39] Arroyo MG, Pérez-Herranz V, Montanes MT, et al. Effect of pH and chloride concentration on the removal of hexavalent chromium in a batch electrocoagulation reactor. *J Hazard Mater.* **2009**;169:1127–1133.
- [40] Villalobos-Lara AD, Álvarez F, Gamiño-Arroyo Z, et al. Electrocoagulation treatment of industrial tannery wastewater employing a modified rotating cylinder electrode reactor. *Chemosphere.* **2021**;264:128491.
- [41] Deveci EÜ, Akarsu C, Gönen Ç, et al. Enhancing treatability of tannery wastewater by integrated process of electrocoagulation and fungal via using RSM in an economic perspective. *Process Biochem.* **2019**;84:124–133.
- [42] Borba F, Seibert D, Pellenz L, et al. Desirability function applied to the optimization of the photoperoxi-electrocoagulation process conditions in the treatment of tannery industrial wastewater. *J Water Process Eng.* **2018**;23:207–216.
- [43] Gong C, Ren X, Han J, et al. Toxicity reduction of reverse osmosis concentrates from petrochemical wastewater by electrocoagulation and Fered-Fenton treatments. *Chemosphere.* **2022**;286:131582.
- [44] Moreno-Casillas HA, Cocke DL, Gomes JA, et al. Electrocoagulation mechanism for COD removal. *Sep Purif Technol.* **2007**;56:204–211.
- [45] Jimenez C, Talavera B, Saez C, et al. Study of the production of hydrogen bubbles at low current densities for electroflotation processes. *J Chem Technol Biotechnol.* **2010**;85:1368–1373.
- [46] Brahmi K, Bouguerra W, Belhsan H, et al. Use of electrocoagulation with aluminum electrodes to reduce

- hardness in Tunisian phosphate mining process water. *Mine Water Environ.* [2016](#);35:310–317.
- [47] Ashraf SN, Rajapakse J, Dawes LA, et al. Electrocoagulation for the purification of highly concentrated brine produced from reverse osmosis desalination of coal seam gas associated water. *J Water Process Eng.* [2019](#);28:300–310.
- [48] Arslan-Alaton I, Kabdaşlı I, Vardar B, et al. Electrocoagulation of simulated reactive dyebath effluent with aluminum and stainless steel electrodes. *J Hazard Mater.* [2009](#);164:1586–1594.
- [49] Kabdaşlı I, Arslan T, Ölmez-Hancı T, et al. Complexing agent and heavy metal removals from metal plating effluent by electrocoagulation with stainless steel electrodes. *J Hazard Mater.* [2009](#);165:838–845.
- [50] Kabdaşlı I, Arslan-Alaton I, Ölmez-Hancı T, et al. Electrocoagulation applications for industrial wastewaters: a critical review. *Environ Technol Rev.* [2012](#);1:2–45.
- [51] Kabdaşlı I, Keleş A, Ölmez-Hancı T, et al. Treatment of phthalic acid esters by electrocoagulation with stainless steel electrodes using dimethyl phthalate as a model compound. *J Hazard Mater.* [2009](#);171:932–940.
- [52] Bhatti MS, Reddy AS, Thukral AK. Electrocoagulation removal of Cr(VI) from simulated wastewater using response surface methodology. *J Hazard Mater.* [2009](#);172:839–846.
- [53] Elabbas S, Ouazzani N, Mandi L, et al. Treatment of highly concentrated tannery wastewater using electrocoagulation: influence of the quality of aluminium used for the electrode. *J Hazard Mater.* [2016](#);319:69–77.
- [54] Oden MK, Sari-Erkan H. Treatment of metal plating wastewater using iron electrode by electrocoagulation process: optimization and process performance. *Process Saf Environ Prot.* [2018](#);119:207–217.
- [55] de Oliveira AG, Ribeiro JP, Neto EFA, et al. Removal of natural organic matter from aqueous solutions using electrocoagulation pulsed current: optimization using response surface methodology. *Water Sci Technol.* [2020](#);82:56–66.
- [56] Ganiyu SO, Martinez-Huitle CA, Rodrigo MA. Renewable energies driven electrochemical wastewater/soil decontamination technologies: a critical review of fundamental concepts and applications. *Appl Catal, B.* [2020](#);270:118857.
- [57] Lu J, Fan R, Wu H, et al. Simultaneous removal of Cr(VI) and Cu(II) from acid wastewater by electrocoagulation using sacrificial metal anodes. *J Mol Liq.* [2022](#);359:119276.
- [58] Kim T, Kim T-K, Zoh K-D. Removal mechanism of heavy metal (Cu, Ni, Zn, and Cr) in the Presence of Cyanide During Electrocoagulation Using Fe and Al Electrodes. *J Water Process Eng.* [2020](#);33:101109.

Table S1. ANOVA results of quadratic model for Cr removal, OPC, EEC, and SSV.

| Source of variations | Sum of square | | | | Degree of freedom | | | | Mean square | | | | F-Value | | | | P-Value Pro.>F | | | |
|-------------------------|---|------------|------------|------------|-------------------|---------------------|-----|-----|-----------------|------------|------------|------------|-----------------|---------|--------|--------|-------------------|---------|---------|---------|
| | R _{Cr} | OPC | EEC | SSV | R _{Cr} | OPC | EEC | SSV | R _{Cr} | OPC | EEC | SSV | R _{Cr} | OPC | EEC | SSV | R _{Cr} | OPC | EEC | SSV |
| Model | 370.02 | 8.515E-004 | 2.260E-004 | 5.697E+005 | 5 | 5 | 5 | 5 | 74.00 | 1.703E-004 | 4.519E-005 | 1.139E+005 | 127.68 | 982.04 | 139.55 | 183.44 | < | < | < | < |
| A-EC time | 30.93 | 3.461E-004 | 6.529E-005 | 66413.49 | 1 | 1 | 1 | 1 | 30.93 | 3.461E-004 | 6.529E-005 | 66413.49 | 53.37 | 1996.01 | 201.63 | 106.93 | 0.0002^ | < | < | < |
| B-Current | 328.66 | 4.497E-004 | 1.383E-004 | 4.909E+005 | 1 | 1 | 1 | 1 | 328.66 | 4.497E-004 | 1.383E-004 | 4.909E+005 | 567.05 | 2593.39 | 426.98 | 790.37 | < | < | < | < |
| AB | 7.40 | 5.329E-005 | 1.794E-005 | 10000.00 | 1 | 1 | 1 | 1 | 7.40 | 5.329E-005 | 1.794E-005 | 10000.00 | 12.76 | 307.31 | 55.40 | 16.10 | 0.0091^ | < | 0.0001* | 0.0051^ |
| A ² | 2.97 | 4.452E-008 | 7.874E-008 | 2238.29 | 1 | 1 | 1 | 1 | 2.97 | 4.452E-008 | 7.874E-008 | 2238.29 | 5.13 | 0.26 | 0.24 | 3.60 | 0.0579 | 0.6279 | 0.6370 | 0.0994 |
| B ² | 0.20 | 2.340E-006 | 4.452E-006 | 311.11 | 1 | 1 | 1 | 1 | 0.20 | 2.340E-006 | 4.452E-006 | 311.11 | 0.35 | 13.50 | 13.75 | 0.50 | 0.5714 | 0.0079^ | 0.0076^ | 0.5020 |
| Residual | 4.06 | 1.214E-006 | 2.267E-006 | 4347.50 | 7 | 7 | 7 | 7 | 0.58 | 1.734E-007 | 3.238E-007 | 621.07 | | | | | | | | |
| Lack of fit | 2.92 | 1.219E-007 | 1.965E-007 | 877.50 | 3 | 3 | 3 | 3 | 0.97 | 4.062E-008 | 6.551E-008 | 292.50 | 3.42 | 0.15 | 0.23 | 0.34 | 0.1331 | 0.9253 | 0.9351 | 0.8008 |
| Pure error | 1.14 | 1.092E-006 | 2.070E-006 | 3470.00 | 4 | 4 | 4 | 4 | 0.28 | 2.730E-007 | 5.176E-007 | 867.50 | | | | | | | | |
| Cor Total | 374.07 | 8.527E-004 | 2.282E-004 | 5.740E+005 | 12 | 12 | 12 | 12 | | | | | | | | | | | | |
| Other parameters | | | | | | | | | | | | | | | | | | | | |
| | R ² /R ² _{adj} /R ² _{pred} (%) | Mean | C.V.% | Press | Adeq Precision | | | | | | | | | | | | | | | |
| R _{Cr} | 0.989/0.981/0.939 | 91.19 | 0.83 | 22.53 | 35.417 | *Highly significant | | | | | | | | | | | | | | |
| OPC | 0.998/0.997/0.997 | 0.014 | 3.03 | 2.573E-006 | 99.506 | ^Significant | | | | | | | | | | | | | | |
| EEC | 0.990/0.983/0.979 | 5.790E-003 | 9.83 | 4.632E-006 | 37.035 | | | | | | | | | | | | | | | |
| SSV | 0.992/0.987/0.979 | 483.85 | 5.15 | 11661.88 | 42.992 | | | | | | | | | | | | | | | |

